European Radiology (2018) 28:2882–2889
https://doi.org/10.1007/s00330-017-5218-9

MUSCULOSKELETAL

Normalized STEAM-based diffusion tensor imaging provides a robust assessment of muscle tears in football players: preliminary results of a new approach to evaluate muscle injuries

Chiara Giraudo[1] · Stanislav Motyka[1] · Michael Weber[1] · Manuela Karner[1] · Christoph Resinger[2] · Thorsten Feiweier[3] · Siegfried Trattnig[1,4] · Wolfgang Bogner[1]

Received: 28 July 2017 / Revised: 27 October 2017 / Accepted: 28 November 2017 / Published online: 8 February 2018

Abstract

Objectives To assess acute muscle tears in professional football players by diffusion tensor imaging (DTI) and evaluate the impact of normalization of data.

Methods Eight football players with acute lower limb muscle tears were examined. DTI metrics of the injured muscle and corresponding healthy contralateral muscle and of ROIs drawn in muscle tears (ROI_{tear}) in the corresponding healthy contralateral muscle (ROI_{hc_t}) in a healthy area ipsilateral to the injury (ROI_{hi}) and in a corresponding contralateral area (ROI_{hc_i}) were compared. The same comparison was performed for ratios of the injured (ROI_{tear}/ROI_{hi}) and contralateral sides (ROI_{hc_t}/ROI_{hc_i}). ANOVA, Bonferroni-corrected post-hoc and Student's t-tests were used.

Results Analyses of the entire muscle did not show any differences ($p>0.05$ each) except for axial diffusivity (AD; $p=0.048$). ROI_{tear} showed higher mean diffusivity (MD) and AD than ROI_{hc_t} ($p<0.05$). Fractional anisotropy (FA) was lower in ROI_{tear} than in ROI_{hi} and ROI_{hc_t} ($p<0.05$). Radial diffusivity (RD) was higher in ROI_{tear} than in any other ROI ($p<0.05$). Ratios revealed higher MD and RD and lower FA and reduced number and length of fibre tracts on the injured side ($p<0.05$ each).

Conclusions DTI allowed a robust assessment of muscle tears in athletes especially after normalization to healthy muscle tissue.

Key Points

- *STEAM-based DTI allows the investigation of muscle tears affecting professional football players.*
- *Fractional anisotropy and mean diffusivity differ between injured and healthy muscle areas.*
- *Only normalized data show differences of fibre tracking metrics in muscle tears.*
- *The normalization of DTI-metrics enables a more robust characterization of muscle tears.*

Keywords Diffusion tensor imaging · Magnetic resonance imaging · Muscle · Injury · Athletes

✉ Chiara Giraudo
chiara_giraudo@hotmail.it

[1] High Field MR Center, Department of Biomedical Imaging and Image-guided Therapy, Medical University of Vienna, Waehringer Guertel 18-20, 1090 Vienna, Austria

[2] Orthopedic Department, Evangelisches Krankenhaus Wien, Vienna, Austria

[3] Siemens Healthcare GmbH, Erlangen, Germany

[4] Christian Doppler Laboratory for Clinical Molecular MR Imaging, Medical University of Vienna, Vienna, Austria

Abbreviations

ROI_{tear}	Region of interest (ROI) drawn on the muscle tear
ROI_{hc_t}	ROI drawn on the corresponding healthy contralateral muscle
ROI_{hi}	ROI drawn on a healthy area ipsilateral to the injury
ROI_{hc_i}	ROI drawn on an area matching with ROI_{hi} on the contralateral limb

Introduction

Acute muscle injuries are very common in elite and non-elite athletes, and tears due to indirect active traumatic events especially have a high prevalence [1, 2]. In the last decades, the

clinical evaluation of muscle strains has increasingly been associated with imaging-based assessment [2, 3]. Several grading systems of muscle injuries have been proposed in the clinical and radiological literature [4–6] and recently the Munich Consensus Statement highly recommended the use of an accurate terminology about muscle lesions [7]. Nevertheless, the prevalent MRI-based classification is still based on a rough quantification of the amount of torn fibres [8] preventing a high imaging-based accuracy in both therapeutic and prognostic management of patients [9]. Diffusion tensor imaging (DTI) [10–12] has been successfully used to investigate muscle tears on an animal model (i.e. dystrophic and wild mice) [13] as well as in patients (i.e. two patients with acute muscle tears) [14]. Even though DTI allows an accurate assessment of muscle anatomy [15–18] and disorders [13, 14, 19–21], it is affected by challenges (i.e. short T2 relaxation times of muscle) [22] and artifacts [23–25]. The development of new techniques for muscle fibre-tracking is, therefore, an active field of research [26–28]. Promising results were recently obtained using a Stimulated Echo Acquisition Mode (STEAM) sequence, which, among other advantages, is hardly affected by eddy current distortions and enables long diffusion times without strong T2-induced signal-to-noise ratio (SNR) loss via the application of mixing time (TM) [25, 29].

Despite the above-mentioned encouraging results and technical improvements, to the best of our knowledge a prospective study applying STEAM-DTI for investigating acute muscle tears in athletes has not been performed yet. Therefore, the main aim of this study was to assess and quantify acute muscle tears affecting the lower limb of professional football players with STEAM-DTI. As it has been demonstrated that in athletes differences between the muscles of the preferred and non-preferred leg occur [30–33], the second aim of this study was to evaluate the impact of a normalization of the data by deriving a ratio between injured and healthy areas on the injured limb and healthy areas on the contralateral extremity.

Materials and methods

Patients and study design

Eight professional football players (all males, age range 20–36 years) with clinically diagnosed acute muscle tears (i.e. < 1 week) of the lower limb were enrolled in this prospective, IRB-approved study. Written informed consent was obtained from each patient.

MR protocol

Each patient was investigated on a 3T MAGNETOM Trio, a Tim system MRI Scanner (Siemens Healthcare, Erlangen, Germany) using a combination of an anterior four-channel matrix coil and a 12-channel spine coil. Both limbs (i.e. the injured and the healthy contralateral) were covered by a single STEAM-DTI scan with the following parameters: repetition time/echo time/TM (TR/TE/TM) 6,100 ms/30 ms/186 ms, 128 × 96 matrix, field of view (FOV) 440 × 330 mm^2, GeneRalized Autocalibrating Partial Parallel Acquisition-2 (GRAPPA-2), diffusion time 200 ms, fat saturation (frequency selective suppression and gradient reversal), b-values 0 and 500 s/mm^2, six averages, 12 directions; 30 adjacent axial slices of 3.5-mm thickness, time of acquisition (TA) 8:10 min; voxel volume 3.4 × 3.4 × 3.5 mm^3.

For the morphological assessment, only the injured limb was imaged via positioning-matched, axial (TR/TE 3,000 ms/26 ms, matrix 384 × 384, FOV 220 × 220mm^2, TA=1:18 min), coronal and sagittal proton density fat-sat (TR/TE 4,600 ms/26 ms, matrix 384 × 384, FOV 400 × 400 mm^2, TA=4:18min, each) and axial T1-weighted TSE (TR/TE 921 ms/11 ms, matrix 448 × 448, FOV 220 × 220 mm^2, TA=4:23 min) with 3-mm slice thickness.

Morphological assessment

Each injury was rated according to the Munich Consensus classification (i.e. minor partial, moderate partial and (sub)total muscle tear/tendinous avulsion) [7] by a musculoskeletal radiologist (C.G., 6 years of experience in musculoskeletal radiology) using all morphological datasets.

DTI post-processing

DTI images with the same contrast were co-registered to correct gross motion artifacts and/or misalignment [25]. Since STEAM-DTI images are affected by random artifacts due to involuntary muscle contractions [23, 25], a recent correction method, based on the weighted mean of voxels' signal intensity (WMSI), was applied [25]. Then, a second co-registration among images from the same slice but with different diffusion gradient directions was used [25].

Masking was performed by multiplying MD and RD maps [25]. Matlab (The Mathworks, Natick, MA, USA) was used for the artifact correction, for both co-registrations and masking.

A fourth-order Runge-Kutta (RK4) tracking algorithm (DSI Studio,http://dsi-studio.labsolver.org) (FA and angular threshold 0.12 and 17°, respectively) [25, 34] was applied.

DTI quantitative evaluation

Entire muscle analyses

DTI metrics (i.e. fractional anisotropy (FA), mean (MD), radial (RD) and axial (AD) diffusivity, number, length and volume of fibre tracts) were collected, after manual segmentation, from

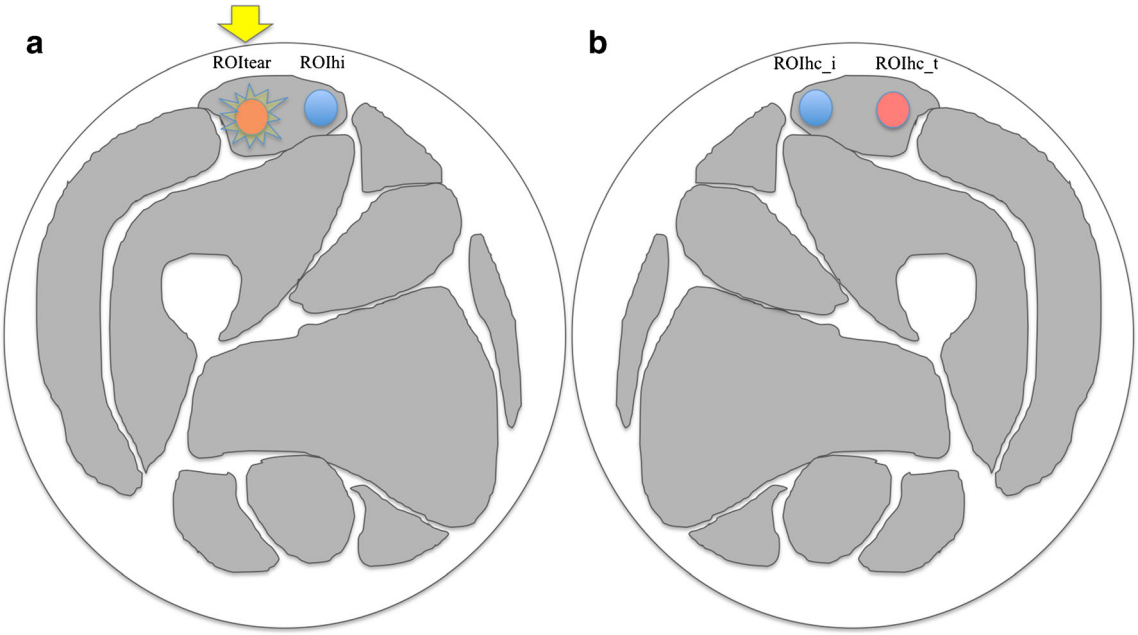

Fig. 1 Drawing of the muscles of the thigh representing the regions of interest (ROIs) used for the ratio analysis. In this example, an injured area on the right rectus femoris muscle is represented (yellow star) where a manual ROI (red ROI in **a**, indicated by the yellow arrow) has been drawn (ROI_{tear}). The same ROI has been drawn on a healthy ipsilateral area (blue ROI in **a**; i.e., ROI_{hi}). The same areas were then investigated on the contralateral side (red and blue ROIs in **b**, respectively ROI_{hc_t} and ROI_{hc_i})

the entire examined section of the injured muscle and from the healthy contralateral corresponding muscle using DSI Studio (i.e. using b0 and PD-FS images in the background as anatomical reference). The contralateral leg was chosen as control, rather than control participants, because of the high inter-subject variability in DTI measurements [35–38].

Region of interest (ROI) analyses

Freehand regions of interest (ROIs) were drawn along the margins of each muscle tear (ROI_{tear}) (i.e. using b0 and PD-FS images in the background as anatomical reference) and the same ROI was applied on the corresponding healthy contralateral muscle (ROI_{hc_t}). To rule out any physiological difference between right and left limbs, two other ROIs were drawn, both in healthy tissue: one in a healthy area ipsilateral to the injury (ROI_{hi}) and one in a matching area in the contralateral limb (ROI_{hc_i}) (Fig. 1).

Ratio

As it has already been demonstrated in the literature, differences between the muscles of the dominant and contralateral limb may occur in professional athletes [30–33]. Thus, to avoid any bias, an intra-subject normalization of DTI metrics was performed: ratios of DTI metrics of the injured side (ROI_{tear}/ROI_{hi}) and of the two corresponding contralateral healthy areas (ROI_{hc_t}/ROI_{hc_i}) were compared.

Statistical analysis

Descriptive statistics were applied for categorical data. One-way repeated measures analysis of variance (ANOVA) with Greenhouse-Geisser correction and Bonferroni post-hoc tests were used to evaluate differences among all the examined ROIs. Student's t-tests were applied to compare DTI metrics of the entire muscles as well as ratios of DTI metrics of the injured side (ROI_{tear}/ROI_{hi}) and of the corresponding contralateral healthy areas (ROI_{hc_t}/ROI_{hc_i}).

Table 1 Demographic and clinical findings of the patients with muscle tears enrolled in the study

Gender		8 males
Age range		20–36 years
Injured muscle		
	Gastrocnemius medialis	2
	Rectus femoris	2
	Semimembranosus	1
	Semitendinosus	1
	Soleus	1
	Biceps femoris	1
Grading[#]	Minor partial tear	2
	Moderate partial	6
	(Sub)Total rupture	/

[#] According to the Munich Consensus' classification

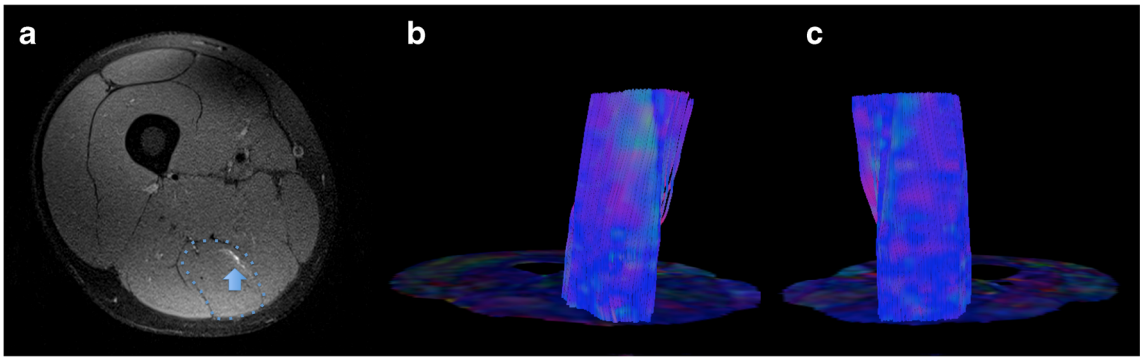

Fig. 2 Axial proton density fat-sat image showing a grade I muscle tear of the right semitendinosus muscle (blue arrow in **a**) of a 20-year-old professional football player. In (**b**) and (**c**), the colour-coded maps of the right and left thigh, respectively, are presented along with the corresponding fibre tracking of both semitendinosus muscles (i.e. blue dotted line in **a**), which do not demonstrate any difference for diffusion tensor imaging (DTI) metrics at the statistical analyses (i.e. Student's t-tests)

All statistical analyses were performed with SPSS Statistics 21.0 (IBM Corp, Armonk, NY, USA), and the level of significance was set at $p<0.05$.

Results

Five out of the eight investigated patients showed an injury of the thigh and three one of the calf. Seven lesions affected the right side and one the left. Two tears were rated as minor partial and six as moderate [7] (Table 1).

DTI quantitative evaluation

Entire muscle

The MD, FA, AD and RD values (mean ± SD) of the injured and corresponding contralateral muscles were 1.35 ± 0.10 ($\times 10^{-3}$ mm^2/s), 0.20 ± 0.06, 1.73 ± 0.16, 1.16 ± 0.09 and 1.30 ± 0.05 ($\times 10^{-3}$ mm^2/s), 0.20 ± 0.05, 1.67 ± 0.12, 1.11 ± 0.05, respectively. The mean ± SD of number, length and volume of the fibre tracts were 8,117 ± 6,348, 44.6 ± 19.2 mm and 93,958 ± 57,292 mm^3 for the injured muscles, and 8,795 ± 6,402, 46.7 ± 20.9 mm, 108,564 ± 66,799 mm^3 for the healthy contralateral. No differences emerged for any of the DTI metrics ($p>0.05$, each) (Fig. 2) except for AD ($p=0.048$) (Table 2).

ROI

ROI analyses allowed an improved characterization of muscle injuries as listed in Table 3. The average volume and amount of voxels of the ROIs were 3,942 ± 2,915mm^3 and 381 ± 282. No differences in DTI metrics were found between ROIs placed in healthy tissue areas ($p>0.05$, each).

The injured areas (i.e. ROI_{tear}) showed higher MD (+10.3% than ROI_{hc_t} and +12.3% than ROI_{hc_i}, respectively; $p<0.05$ each) and higher AD values (+6.6% than ROI_{hc_t} and +9.1% than ROI_{hc_i}, respectively; $p<0.05$, each) than the contralateral healthy areas. There were no differences compared to the ipsilateral healthy regions (i.e. ROI_{hi}) ($p>0.05$ for each DTI metric).

Table 2 Entire muscle analyses. Comparison between the injured muscle and the contralateral corresponding healthy muscle

	Entire muscle with tear (mean ± SD)	Entire contralateral healthy muscle (mean ± SD)	Student's t-test *p* value*
tr_n	8116 ± 6347	8794 ± 6402	0.396
tr_l (mm)	44.6 ± 19.16	46.74 ± 20.85	0.496
tr_v (mm^3)	93,957.61 ± 57,291.74	108,564.36 ± 66,799.11	0.189
FA	0.20 ± 0.06	0.20 ± 0.05	0.858
MD (10^{-3}mm^2/s)	1.35 ± 0.10	1.30 ± 0.05	0.078
AD	1.73 ± 0.16	1.67 ± 0.11	**0.048**
RD	1.16 ± 0.09	1.11 ± 0.05	0.106

tr_n number of tracks, *tr_l* length of tracks, *tr_v* volume of tracks, *FA* fractional anisotropy, *MD* mean diffusivity, *AD* axial diffusivity, *RD* radial diffusivity

*Bold type indicates statistically significant values ($p<0.05$)

Table 3 Region of interest (ROI)-based diffusion tensor imaging (DTI) analyses

	ROI_{tear}	ROI_{hc_t}	ROI_{hi}	ROI_{hc_i}	1-Way ANOVA (*P*)	*Post-hoc tests*^					
						ROI_{tear} vs. ROI_{hc_t}	ROI_{tear} vs. ROI_{hi}	ROI_{tear} vs. ROI_{hc_i}	ROI_{hc_t} vs. ROI_{hi}	ROI_{hc_t} vs. ROI_{hc_i}	ROI_{hi} vs. ROI_{hc_i}
tr_n	972 ± 997	1,633 ± 1317	1,002 ± 669	893 ± 661	0.182	-	-	-	-	-	-
tr_l (mm)	37.30 ± 22	54.15 ± 24.83	48.08 ± 23.1	44.10 ± 23.7	**0.043**	0.065	0.596	1.000	1.000	0.366	1.000
tr_v (mm^3)	14,530 ± 13,925	22,424 ± 12,960	14,371 ± 10,191	13,482 ± 11,349	0.102	-	-	-	-	-	-
FA	0.18 ± 0.05	0.20 ± 0.04	0.22 ± 0.05	0.20 ± 0.04	**0.008**	**0.018**	**0.015**	0.098	0.454	1.000	1.000
MD ($10^{-3}mm^2/s$)	1.44 ± 0.11	1.31 ± 0.07	1.33 ± 0.13	1.28 ± 0.1	**0.002**	**0.003**	0.084	**0.002**	1.000	1.000	1.000
AD	1.8 ± 0.15	1.7 ± 0.15	1.7 ± 0.18	1.65 ± 0.17	**0.001**	**0.007**	0.336	**0.007**	1.000	0.784	0.282
RD	1.27 ± 0.12	1.12 ± 0.07	1.14 ± 0.13	1.10 ± 0.08	**0.003**	**0.005**	**0.047**	**0.003**	1.000	1.000	1.000

Comparison between the muscle tear and the healthy contralateral and ipsilateral muscle areas

tr_n number of tracks, tr_l length of tracks, tr_v volume of tracks, *FA* fractional anisotropy, *MD* mean diffusivity, *AD* axial diffusivity, *RD* radial diffusivity

ROI_{tear} region of interest drawn on the muscle tear, ROI_{hc_t} ROI drawn on the on the corresponding healthy contralateral muscle, ROI_{hi} ROI drawn on a healthy area ipsilateral to the injury, ROI_{hc_i} ROI drawn on an area matching the ROI_{hi} on the contralateral limb, ^ Greenhouse Geisser

Bold type indicates statistically significant values ($p<0.05$)

Also concerning FA, the differences were inhomogeneous. Even if FA was lower in the injured areas (i.e. ROI_{tear}) than in the ipsilateral healthy ones (-19.8 % than in ROI_{hi}; $p=0.002$) (Fig. 3), differences in the contralateral side emerged only with the healthy ROIs specular to the tear (-11.5 % than in ROI_{hc_t}; $p=0.003$). No differences of FA were found between tears (ROI_{tear}) and contralateral areas corresponding to the healthy ROI on the injured side (ROI_{hc_i}; $p>0.05$).

RD was higher in muscle tears than in any other examined ROIs (+13.1 % than ROI_{hc_t}, +10.5 % than ROI_{hi}, and +14.8 % than ROI_{hc_i}; $p<0.05$).

There were no differences for number, length and volume for fibre tracts in any of the performed comparisons ($p>0.05$, each) (Fig. 4).

Ratio

The differences between healthy and injured muscles, particularly the fibre-tracking parameters, were more pronounced after normalization (Table 4). Comparison of the ratios (ROI_{tear}/ROI_{hi} and ROI_{hc_t}/ROI_{hc_i}) revealed higher MD and RD (+6 % and +8.7 %, respectively; $p<0.05$ each) and lower FA (-19.5 %, $p=0.07$) as well as a reduced number and length of fibre tracts on the injured side (-55.6 % and -39.5 %, respectively; $p<0.05$) (Fig. 4). There were no differences for AD and fibre tract volume ($p>0.05$, each).

Discussion

Our results suggest that normalized DTI/fibre-tracking metrics obtained via artifact-corrected STEAM-DTI are insensitive to possible bias due to laterality, being thus well suited for quantitative diagnostic assessment of muscle tears.

Acute muscle tears are characterized by alterations of the myofibrillar structure and inflammation [39, 40]. DTI is uniquely sensitive to changes in the magnitude and directionality of intramuscular water diffusivity occurring in acute muscle tears. Hence, these alterations are expected to be easily detected and quantified by this technique. Our results show an absence of significant differences (i.e. besides higher AD on the injured side) comparing entire and injured muscles. This is consistent with observations by McMillan et al. on an animal model for injuries of the tibialis anterior [13]. Indeed, these authors found significant differences in DTI metrics only comparing wild and dystrophic mice with muscle injury or comparing injured and non-injured dystrophic animals, whereas differences between injured and non-injured wild animals did not occur [13].

In contrast, Zaraiskaya et al. [14] showed significant differences in FA, MD and eigenvalues (i.e. $\lambda_1,\lambda_2,\lambda_3$) comparing DTI measures from entire healthy muscles (i.e. eight volunteers) with those obtained in ROIs drawn in injured muscle

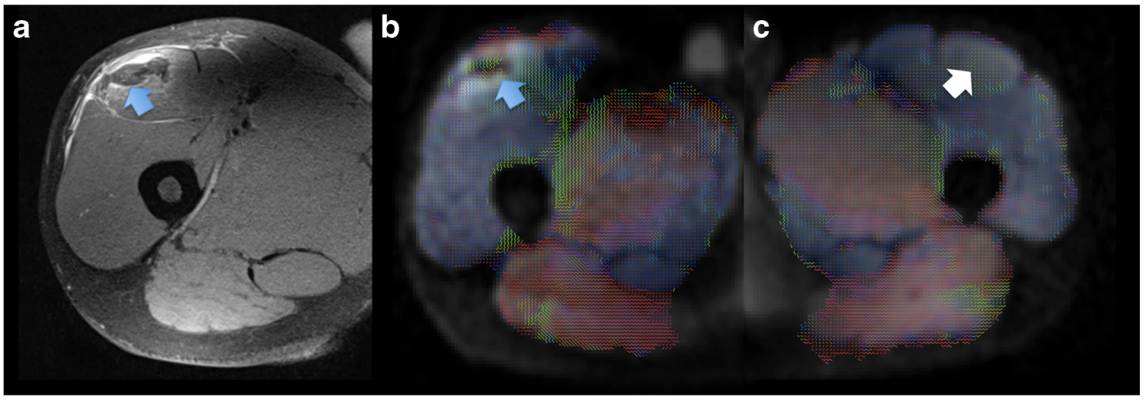

Fig. 3 Grade II muscle tear of the right rectus femoris muscle (blue arrow on the axial proton density fat-saturated image in **a**) of a 23-year-old professional football player. The injured area demonstrates lower fractional anisotropy (FA) (blue arrow on the FA map in **b**) than the corresponding healthy contralateral muscle (white arrow on the FA map in **c**)

areas of the calves of four patients (i.e. two with haematomas and two with muscle tears). These results are in accordance with the differences in FA, MD, RD and AD found in our population comparing the injured areas with the healthy ones (i.e. ipsi- and contralateral ROIs), even if it has to be taken into account that the presence of oedema may lead just to an apparent decrease of AD and FA [41].

Zaraiskaya et al. performed fibre tracking only in healthy controls, but no such data were presented for patients [14]. Froeling et al. [35] evaluated fibre-tracking changes at different time points in marathon runners, but performed no separate assessments for muscle strains already visible on anatomical images (i.e. T2w images). To the best of our knowledge, there are no previous studies that have investigated fibre-tracking metrics (i.e. number, length and volume of tracked fibres) of muscle tears. In our cohort, no differences in fibre tracking emerged, either in the entire muscle, or in the ROI-based analyses. The tracked muscle fibres of the injured side turned out to be significantly less numerous (-55 %) and shorter (-39 %) only after normalization of the data. Considering that in athletes an asymmetry in the characteristics and metabolic activity of muscle belonging to the dominant and non-dominant side has been shown [30–33], it appears reasonable that the laterality is a biasing factor in quantitative DTI assessments in muscles. The results obtained after applying the normalization seem to confirm this assumption, as differences in length, number and volume of the tracked fibres due to the injury were apparent only in normalized data.

Our study results are preliminary and could not yet validate the fact that STEAM-DTI brings any additional benefits compared to conventional MRI. Since one of the more challenging aspects of muscle tear assessment is represented by the prognosis of the recovery interval [42], we strongly believe that the application of the ratio could also provide essential benefits for the longitudinal evaluation of muscle strains during the recovery phase and thus improve the prediction of the recovery interval and reduce the risk of recurrence.

Limitations

Despite our very promising results, there are some limitations to our study. All patients were scanned within 1 week after the

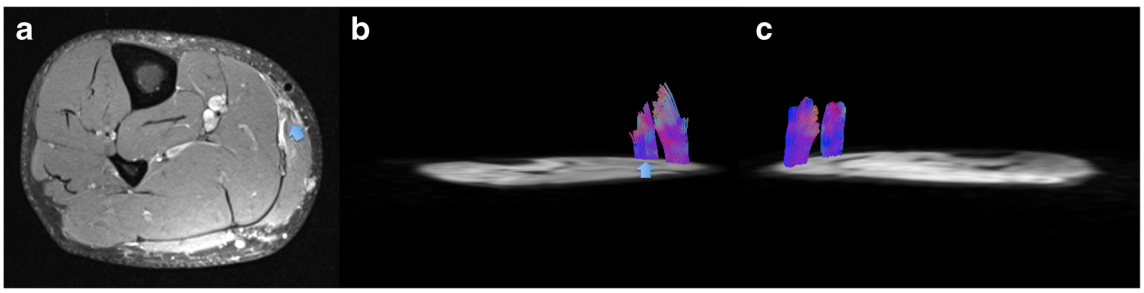

Fig. 4 Grade II lesion of the right medial gastrocnemius (blue arrow on the axial proton density fat-saturated image in **a**) of a 35-year-old football player. Fibre tracking of the injured area is illustrated (blue arrow in **b**) and of the ipsi- (**b**) and contralateral healthy areas (**c**). Although visually the fibre tracking of the injured muscle area seems to demonstrate shorter and less numerous fibres, no statistically significant differences occurred in our population comparing the tears with all healthy areas. The statistical analyses revealed significant differences in terms of length and amount of fibre tracts only when a ratio between the ROIs on the injured (i.e. represented here by the fibre tracts on the right calf in **b**) and contralateral extremity (i.e. represented here by the fibre tracts on the left calf in **c**) was calculated

Table 4 Comparison of diffusion tensor imaging (DTI) metrics' ratio between the injured leg and the contralateral healthy one

	ROI_{tear}/ROI_{hi}	ROI_{hc_t}/ROI_{hc_i}	Students' t-test
tr_n	0.55 ± 0.45	1.24 ± 0.53	**0.028**
tr_l (mm)	0.69 ± 0.22	1.14 ± 0.28	**0.005**
tr_v (mm^3)	0.62 ± 0.40	1.26 ± 0.65	0.056
FA	0.88 ± 0.07	1.09 ± 0.15	**0.007**
MD ($10^{-3}mm^2/s$)	1.10 ± 0.04	1.04 ± 0.07	**0.028**
AD	1.06 ± 0.03	1.04 ± 0.04	0.241
RD	1.13 ± 0.06	1.03 ± 0.10	**0.014**

tr_n number of tracks, tr_l length of tracks, tr_v volume of tracks, *FA* fractional anisotropy, *MD* mean diffusivity, *AD* axial diffusivity, *RD* radial diffusivity, ROI_{tear}/ROI_{hi} ratio between the ROI drawn on the tear and the one drawn on a ipsilateral healthy area, ROI_{hc_t}/ROI_{hc_i} ratio of the two corresponding contralateral healthy areas

Bold type indicates statistically significant values ($p<0.05$)

injury; however, DTI/fibre-tracking metrics may change quite quickly (e.g. inflammation may occur in a few days). Thus, a more standardized recruitment (i.e. a fixed number of days after the injury for all patients) may be beneficial, especially for entire muscle analyses. Despite the evidence that in volunteers different ranges of DTI metrics values occur in different muscles [15, 16], in the present study separate analyses according to the injured muscles were not performed, because of the low number of examined patients. Future studies including larger patient populations should focus on muscle-specific analyses to provide even more accurate results. Nevertheless, normalization will certainly also reduce such differences between muscle groups.

Finally, the quite long acquisition time (i.e. ca. 8 min) might represent a limit with very extensive lesions, since motion artifacts may occur. However, recent developments in simultaneous-multi-slice (SMS) DTI have translated into ~threefold acceleration of clinically available DTI sequences [43]. SMS was not yet implemented into our STEAM-DTI sequence when our study was performed, but future studies aiming for larger FOVs should directly benefit from this new technology.

Conclusion

In conclusion, STEAM-based DTI allowed a precise assessment of the injured fibres in athletes especially when a ratio between the injured and the contralateral muscles was applied. Aiming to improve the current imaging-based classification of muscle tears and to increase the accuracy of the therapeutic and prognostic management of injured athletes, future studies including a larger population and evaluating muscle tears, also during follow-up, are necessary.

Acknowledgements The preliminary results of this study have been presented as an electronic poster at the ISMRM 25th Annual Meeting & Exhibition (22–27 April 2017, Hawaii, USA).

Funding Stanislav Motyka was supported by the OeNB Jubilaeumsfond (Grant #16133) and Giraudo Chiara by the Austrian Science Fund (FWF; Project KLIF 382). Open Access Funding provided by Medical University of Vienna.

Compliance with ethical standards

Guarantor The scientific guarantor of this publication is Prof. Wolfgang Bogner.

Conflict of interest Thorsten Feiweier is senior researcher at Siemens Healthcare GmbH (Siemens, Germany).

The other authors of this manuscript declare no relationships with any companies whose products or services may be related to the subject matter of the article.

Statistics and biometry Michael Weber, co-author of this manuscript, has significant statistical expertise.

Informed consent Written informed consent was obtained from all subjects (patients) in this study.

Ethical approval Institutional Review Board approval was obtained.

Methodology
- prospective
- experimental
- performed at one institution

References

1. Page P (1995) Pathophysiology of acute exercise-induced muscular injury: clinical implications. J Athl Train 30:29–34
2. Lee JC, Mitchell AWM, Healy JC (2012) Imaging of muscle injury in the elite athlete. Br J Radiol 85:1173–1185
3. Cross TM, Gibbs N, Dip G et al (2004) Acute quadriceps muscle strains. Magnetic Resonance Imaging features and prognosis. Am J Sports Med 32:710–719
4. O'Donoghue DO (1962) Treatment of injuries to athletes. WB Saunders, Philadelphia
5. Ryan AJ (1969) Quadriceps strain, rupture and charlie horse. Med Sci Sports 1:106–111
6. Takebayashi S, Takasawa H, Banzai Y et al (1995) Sonographic findings in muscle strain injury: clinical and MR imaging correlation. J Ultrasound Med 14:899–905
7. Mueller-Wohlfahrt HW, Haensel L, Mithoefer K et al (2013) Terminology and classification of muscle injuries in sport: The Munich consensus statement. Br J Sports Med 47:342–350
8. Pedowitz R, Chung CB, Resnick D (2009) Muscle. In Magnetic Resonance Imaging in Orthopedic Sports Medicine. Springer-Verlag GmbH

9. Hamilton B, Valle X, Rodas G et al (2015) Classification and grading of muscle injuries: a narrative review. Br J Sports Med 49:306
10. Alexander AL, Lee JE, Lazar M et al (2007) Diffusion Tensor Imaging of the Brain. Neurotherapeutics 4:316–329
11. Li K, Dortch RD, Brian E et al (2014) Multi-parametric MRI Characterization of Healthy Human Thigh Muscles at 3.0T - Relaxation, Magnetization Transfer, Fat/Water, and Diffusion Tensor Imaging. NMR Biomed 27:1070–1084
12. Scheel M, von Roth P, Winkler T et al (2013) Fiber type characterization in skeletal muscle by diffusion tensor imaging. NMR Biomed 10:1220–1224
13. McMillan A, Shi D, Pratt S et al (2011) Diffusion Tensor MRI to Assess Damage in Healthy and Dystrophic Skeletal Muscle after Lengthening Contractions. J Biomed Biotechnol 970726
14. Zaraiskaya T, Kumbhare D, Noseworthy M (2006) Diffusion Tensor Imaging in evaluation of human skeletal muscle injury. J Magn Reson Imaging 24:402–408
15. Sinha S, Sinha U, Edgerton VR (2006) In vivo diffusion tensor imaging of the human calf muscle. J Magn Reson Imaging 24: 182–190
16. Budzik JF, Le Thuc V, Demondion X et al (2007) In vivo MR tractography of thigh muscles using diffusion imaging: initial results. Eur Radiol 17:3079–3085
17. Kermarrec E, Budzik JF, Khalil C et al (2010) In vivo diffusion tensor imaging and tractography of human thigh muscles in healthy subjects. AJR Am J Roentgenol 195:352–356
18. Froeling M, Nederveen AJ, Heijtel DF et al (2012) Diffusion-tensor MRI reveals the complex muscle architecture of the human forearm. J Magn Reson Imaging 36:237–248
19. Ponrartana S, Ramos-Platt L, Wren TA et al (2015) Effectiveness of diffusion tensor imaging in assessing disease severity in Duchenne muscular dystrophy: preliminary study. Pediatr Radiol 45:582–589
20. Sigmund EE, Sui D, Ukpebor O et al (2013) Stimulated echo diffusion tensor imaging and SPAIR T2-weighted imaging in chronic exertional compartment syndrome of the lower leg muscles. J Magn Reson Imaging 38:1073–1082
21. Budzik JF, Balbi V, Verclytte S (2014) Diffusion tensor imaging in musculoskeletal disorders. Radiographics 34:56–72
22. Schick F, Eismann B, Jung WI et al (1993) Comparison of localized proton NMR signals of skeletal muscle and fat tissue in vivo: two lipid compartments in muscle tissue. Magn Reson Med 29:158–167
23. Steidle G, Schick F (2015) Addressing spontaneous signal voids in repetitive single-shot DWI of musculature: spatial and temporal patterns in the calves of healthy volunteers and consideration of unintended muscle activities as underlying mechanism. NMR Biomed 28:801–810
24. Chang LC, Walker L, Pierpaoli C (2012) Informed RESTORE: a method for robust estimation of diffusion tensor from low redundancy datasets in the presence of physiological noise artifacts. Magn Reson Med 68:1654–1663
25. Giraudo C, Motyka S, Weber M et al (2017) Weighted Mean of Signal Intensity for Unbiased Fiber Tracking of Skeletal Muscles: Development of a New Method and Comparison With Other Correction Techniques. Invest Radiol 52:488–497
26. Saupe N, White LM, Sussman MS (2008) Diffusion tensor magnetic resonance imaging of the human calf: comparison between 1.5 T and 3.0 T-preliminary results. Invest Radiol 43:612–618
27. Karampinos DC, Banerjee S, King KF et al (2012) Considerations in high-resolution skeletal muscle diffusion tensor imaging using single-shot echo planar imaging with stimulated-echo preparation and sensitivity encoding. NMR Biomed 25:766–778
28. Filli L, Piccirelli M, Kenkel D et al (2015) Simultaneous multislice echo planar imaging with blipped controlled aliasing in parallel imaging results in higher acceleration. A promising technique for accelerated diffusion tensor imaging of skeletal muscle. Invest Radiol 50:456–463
29. Noehren B, Andersen A, Feiweier T et al (2015) Comparison of twice refocused spin echo versus stimulated echo diffusion tensor imaging for tracking muscle fibers. J Magn Reson Imaging 41:624–632
30. Rahnama N, Lees A, Bambaecichi E (2005) Comparison of muscle strength and flexibility between the preferred and non-preferred leg in English soccer players. Ergonomics 48:1568–1575
31. Kearns CF, Isokawa M, Abe T (2001) Architectural characteristics of dominant leg muscles in junior soccer players. Eur J Appl Physiol 85:240–243
32. Zoladz JA, Kulinowski P, Zapart-Bukowska J et al (2007) Phosphorylation potential in the dominant leg is lower, and [ADPfree] is higher in calf muscles at rest in endurance athletes than in sprinters and in untrained subjects. J Physiol Pharmacol 58: 803–819
33. Hides J, Fan T, Stanton W et al (2010) Psoas and quadratus lumborum muscle asymmetry among elite Australian Football League players. Br J Sports Med 44:563–567
34. Basser PJ, Pajevic S, Pierpaoli C et al (2000) In vivo fiber tractography using DT-MRI Data. Magn Reson Med 44:625–632
35. Froeling M, Oudeman J, Strijkers GJ et al (2015) Muscle changes detected with diffusion-tensor imaging after long-distance running. Radiology 274:548–562
36. Lansdown DA, Ding Z, Wadington M et al (1985) (2007) Quantitative diffusion tensor MRI-based fiber tracking of human skeletal muscle. J Appl Physiol 103:673–668
37. Okamoto Y, Kunimatsu A, Kono T et al (2010) Gender differences in MR muscle tractography. Magn Reson Med Sci 9:111–118
38. Galbán CJ, Maderwald S, Stock F et al (2007) Age-related changes in skeletal muscle as detected by diffusion tensor magnetic resonance imaging. J Gerontol A Biol Sci Med Sci 62:453–458
39. Fernandes TL, Pedrinelli A, Hernandes AJ (2011) Muscle injury – physiopathology, diagnosis, treatment and clinical presentation. Rev Bras Ortop 46:247–255
40. Delos D, Maak TG, Rodeo SA (2013) Muscle Injuries in Athletes: Enhancing Recovery Through Scientific Understanding and Novel Therapies. Sports Health 5:346–352
41. Froeling M, Nederveen AJ, Nicolay K et al (2013) DTI of human skeletal muscle: the effects of diffusion encoding parameters, signal-to-noise ratio and T2 on tensor indices and fiber tracts. NMR Biomed 26:1339–1352
42. Slavotinek JP (2010) Muscle Injury: The Role of Imaging in Prognostic Assignment and Monitoring of Muscle Repair. Semin Musculoskelet Radiol 14:194–200
43. Setsompop K, Cohen-Adad J, Gagoski BA et al (2012) Improving diffusion MRI using simultaneous multi-slice echo planar imaging. NeuroImage 63:569–580